

# Impact of Battery Degradation on Thermal Runaway Risks in Lithium-Ion Batteries: a Statistical and Modelling Approach

Milad Tulabi\*, Roberto Bubbico

Department of Chemical Material and Environmental Engineering, "Sapienza" Rome University, Via Eudossiana 18, 00184, Rome, Italy

[milad.tulabi@uniroma1.it](mailto:milad.tulabi@uniroma1.it)

Li-ion batteries are commonly used in an increasing number of applications, but they are characterized by different safety problems connected with their operating temperature. In fact, depending on the balance between the heat internally produced during operation and that dissipated towards the external environment, a thermal runaway can occur beyond certain values of the internal temperature, with possible dangerous events, such as fires and explosions. While most existing research investigates TR in new or minimally cycled batteries, real-world TR incidents predominantly occur in aged batteries, underscoring the need for a targeted investigation into the aging effects. This study will examine the effect of battery degradation on the likelihood of thermal runaway (TR) events, with a focus on the main degradation parameters that impact thermal behavior in lithium-ion batteries (LIBs), such as internal resistance, the charge/discharge current, and the cell capacity. A mathematical model was developed and validated against established literature, allowing for a detailed statistical analysis of each parameter's influence on TR. Preliminary results indicate that charge/discharge current is the most significant contributor, showing the lowest p-value with confident level of 95% in relation to temperature increases at a state of charge (SOC) of 50%. The findings of this study will enhance understanding of TR risks in aged LIBs and provide a foundation for improved battery management strategies to mitigate safety hazards in degraded batteries.

## 1. Introduction

Energy production, particularly from fossil fuels, is the primary source of global greenhouse gas emissions and air pollution (Wang and Azam, 2024), contributing to millions of deaths each year. The current reliance on fossil fuels is increasingly problematic due to rising demand, depletion of resources, and geopolitical instability. To address climate change and cut CO<sub>2</sub> emissions, a transition to low-carbon energy sources like wind and solar power is crucial. Effective energy storage solutions, such as batteries and supercapacitors, are needed to manage the variability of renewable energy and maintain a consistent power supply. Additionally, adopting electric and hybrid vehicles can play a significant role in reducing emissions in the transportation sector. Lithium-ion batteries are a type of secondary battery that is usually used for portable electronic devices and electric cars, and every day they are getting more popular for use in various industries.

The safety of lithium-ion batteries is heavily influenced by the failure of individual components, or the integrity of the battery system. These vulnerabilities become pronounced under various abusive conditions, including but not limited to overcharging, which can lead to Thermal Runaway (TR) and subsequent catastrophic failure, dendritic lithium growth within the cell, causing internal short circuits, dissolution of current collectors compromising electrical conductivity, and the evolution of gas, potentially leading to pressure build-up and rupture (Bubbico et al., 2018). These factors collectively contribute to the intricate safety challenges inherent in lithium-ion battery technology (Wen et al., 2012). Thermal runaway involves a chain reaction mechanism triggered by abnormal temperature increases in Li-ion cells under abusive conditions. This process is fueled by the Heat-Temperature-Reaction (HTR) loop. Initially, abnormal heat generation raises the cell's temperature, initiating side reactions like the decomposition of the solid electrolyte interface (SEI). These reactions release additional heat, perpetuating the HTR loop until the cell undergoes Thermal Runaway (Feng et al. 2018).

Reactions leading to thermal runaway can be categorized based on the area where they happen: anode reactions, cathode reactions and electrolyte decompositions.

Battery models developed over the years. Doyle and Newman (Doyle et al., 1993, Doyle et al., 1996) studied modeling of Li-ion batteries and their work is the basis of many afterward studies. Doyle et al. (1996) compares modeling predictions with experimental data from plastic lithium-ion cells, focusing on discharge curves, resistance profiles, and parameter optimizations. They discuss the impact of electrode thickness, film resistance, and diffusion limitations on battery performance and highlight the importance of accurate parameter values and design optimization for enhancing specific energy and power capabilities in lithium-ion batteries. These models typically function in a one-dimensional manner across the battery cell layers, adding an additional dimension to represent solid lithium diffusion within the electrode particles. This is known as a "pseudo-2D" (P2D) approach. However, setting up such a model generally requires around 40 parameters, making it impractical for engineering applications where detailed knowledge of the internal battery chemistry might be limited. For low to moderate currents, and to improve computational efficiency without sacrificing accuracy, the Newman model can be simplified using a single-particle (SP) approach. The SP model simplifies the process by ignoring the detailed distribution of local concentration and potential in the solution phase, instead using a lumped solution resistance term. Additionally, it assumes that local reaction currents across the porous electrode are constant, treating the porous electrode as a collection of single particles all under the same conditions. These assumptions are valid for low applied current densities, thin electrodes, and highly conductive electrodes, where overpotential is primarily influenced by solid-state diffusion. At high current densities, concentration gradients in the electrolyte become significant. The SP model does not account for these concentration gradients and is therefore limited to low to moderate current densities (Guo et al, 2012).

Modeling thermal runaway in lithium-ion batteries is a critical area of research aimed at understanding and mitigating safety risks associated with battery operation (Ciancullo et al., 2022). Another significant aspect is the incorporation of thermal abuse models, which simulate extreme conditions such as overcharging or external heating to predict how these conditions can trigger thermal runaway. In the wake of a previous study (Menale et al., 2019), the present analysis is focused on the main influential factors on temperature of a cell in an aged cell.

## 2. Methodology

The main aim of this study is to develop an electrochemical-thermal model which predict the behavior of an aged cell. In the following section, the energy and mass balances governing this model are discussed.

### 2.1 Energy Balance

The following is the energy balance equation used in the system:

$$\frac{\partial(\rho c_p T)}{\partial t} = -\nabla(k\nabla T) + S \quad (1)$$

When Temperature is increasing, side reactions will happen. Four side reactions are: the SEI decomposition reaction (SEID), negative electrode-electrolyte reaction (NE), two positive electrode-electrolyte reactions (PE) (Kim et al., 2007). Heat source terms related to the above reactions are shown in Eq (2), where  $S_{SEI}$  is the heat source for SEI decomposition,  $S_{ne}$  is the heat source for NE,  $S_{pe}$  is the heat source for PE:

$$S = S_{SEI} + S_{ne} + S_{pe} \quad (2)$$

For simplicity, a 2D geometry with axial symmetry feature will be investigated. The Li-ion battery in this study is modeled after a commercial 18650 NCM/graphite battery which has a length of 65 mm, a radius of 9 mm, a container thickness of 0.25 mm, and a mandrel thickness of 2 mm.

For solving the energy balance, these assumptions were made: at  $t=0$  (beginning of the study), the battery and surrounding area are at steady state and the temperature equals 298.15 K; at  $r=R$  (the maximum point with respect to radius), at  $z=0$ , and  $z=L$ , heat transfers to ambient, meaning heat conducted will be released to ambient with natural convection with a heat transfer coefficient of 10 W/m<sup>2</sup>K.

Due to differences in active material with respect to battery parts and lumped assumption of the battery itself, thermal properties of global active material should be calculated. This formulation is shown in Eq (3) and Eq (4):

$$k_{T,r} = \frac{\sum L_i}{\sum L_i / k_{T,i}} \quad (3)$$

$$k_{T,ang} = \frac{\sum L_i k_{T,i}}{\sum L_i} \quad (4)$$

For other thermal properties, the same equations can be used. As mentioned before, when the temperature is rising, exothermic side reactions will happen:

$$R_i = A_i \exp\left(-\frac{E_{a,i}}{RT}\right) c_i^{n_{i,1}} (1 - c_i)^{n_{i,2}} \quad (5)$$

$$S_i = H_i W_i R_i \quad (6)$$

$$\frac{dc_i}{dt} = \begin{cases} R_i, & \text{for PE} \\ -R_i, & \text{for others} \end{cases} \quad (7)$$

The parameters for solving the energy balance and for calculating the heat generated by these reactions are extracted from reference study of Guo et al. (2023).

## 2.2 Mass Balance and Electrochemical Reactions

To simplify and expedite the thermal management calculations for Li-ion batteries, the assumption of a lumped battery model will be used. In the Single-Particle (SP) model, electrodes are represented by spherical intercalation particles of uniform size, assuming a uniform current distribution across the thickness of the porous electrode. Also, at high current densities, concentration gradients in the electrolyte become significant. This model does not account for these concentration gradients; thus, it is suitable only for low to moderate current densities (Guo et al., 2010). Mass balance is presented in Eq (8) with initial conditions of Eq (9).

$$\frac{\partial c_{a,j}}{\partial t} + \frac{15D_{1,j}}{R_j^2} (c_{s,j} - \bar{c}_{1,j}) = 0 \quad (8)$$

$$\frac{15D_{1,j}}{R_j} (\bar{c}_{1,j} - c_{s,j}) + \frac{J_j}{A_j F} = 0 \quad (9)$$

$$c_{s,j}|_{t=0} = c_{1,j,0} \quad (9)$$

The battery cell voltage  $E_{cell}$  is defined as in Eq (10) (Ekström et al., 2018)

$$E_{cell} = E_{OCV}(SOC_{average}) + \eta_{IR} + \eta_{act} + \eta_{conc} \quad (10)$$

Fickian diffusion of a dimensionless SOC variable is solved for in a 1D pseudo extra dimension corresponding to the particle dimension of length 1 with X as the dimensionless spatial variable, using spherical symmetry (for spherical particles), according to Eq (11):

$$\tau \frac{\partial SOC}{\partial t} = -\nabla \cdot (-\nabla SOC) \quad (11)$$

The interval represents an average particle of the electrode governing the battery, where  $X = 0$  and  $X = 1$  represent the center and surface of the particle, respectively. The boundary conditions are as follows:

$$\nabla SOC = 0|_{X=0} \quad (12)$$

$$\nabla SOC = \frac{\tau I_{cell}}{N_{shape} Q_{cell,0}} \Big|_{X=1}$$

Where  $N_{shape}$  is 3 for spherical particles. The surface state-of-charge,  $SOC_{surface}$ , is defined at the surface of the particle ( $X = 1$ ). The average state-of-charge,  $SOC_{average}$ , is defined by integrating over the volume of the particle, appropriately considering spherical coordinates, and defined by Eq (13):

$$SOC_{average} = \frac{\int_0^1 SOC 4\pi X^2 dX}{\int_0^1 4\pi X^2 dX} = 3 \int_0^1 SOC X^2 dX \quad (13)$$

$I_{1C}$ , the current at 1C rate can be calculated by Eq (14):

$$I_{1C} = \frac{Q_{cell,0}}{3600} \quad (14)$$

$R_{ohm}$  (ohmic resistance) is a specific type of resistance that obeys Ohm's Law and excludes any reactive components. It is generally constant across frequencies and provides a purely resistive behavior. The lumped voltage loss associated with ohmic process in the electrolyte and electrodes is given by Eq (15):

$$\eta_{IR} = \eta_{IR,1c} \frac{I_{cell}}{I_{1C}} = R_{ohm} I_{cell} \quad (15)$$

The dimensionless charge exchange current  $J_0$  is used to define the lumped voltage loss associated with the charge transfer reactions (activation overpotential) on both the positive and negative electrode surfaces:

$$\eta_{act} = \frac{2RT}{F} \sinh^{-1} \left( \frac{I_{cell}}{2J_0 I_{1C}} \right) \quad (16)$$

and the lumped voltage loss associated with concentration overpotential is defined as

$$\eta_{conc} = E_{OCV}(SOC_{surface}) - E_{OCV}(SOC_{average}) \quad (17)$$

According to literature (Vetter et al., 2005), after undergoing many charge-discharge cycles, batteries experience degradation, which manifests itself as a decrease in capacity and an increase in internal resistance. From Eq (14) and Eq (15), Eq (18) can be derived

$$\eta_{IR,1c} = R_{ohm} \frac{Q_{cell,0}}{3600} \quad (18)$$

For investigation of degradation leading to increment of impedance,  $R_{ohm}$  can be used. Therefore, for this study, response surface methodology with three 2-level factors and one central point on capacity, ohmic resistance and charging rate will be tested. Charging rates included a base rate of 1C and a high rate of 8C, with capacities of 3 Ah and 0.5 Ah, respectively. Additionally, resistances of 30 micro-ohms and 5 micro-ohms were selected. For assessing the behavior of the cell, the mean temperature of the cell in a 50% charged battery is selected. The results from this design of experiments investigate the influence of the independent parameters using p-score. The model is simulated in Comsol Multiphysics and statistical analysis in Python.

### 3. Results and discussions

The proposed model has been first tested against experimental data from the literature (Dong et al., 2018) providing values of the temperature under different charging/discharging rates. In the experiments the temperature monitoring point is set at the center of the cell cathode outer surface and in the simulation, outer surface temperature at the center is recorded. Figure 1 presents a comparison between simulated and experimental cell temperatures during the 1C and 8C charging processes with initial SOC of nearly zero (0.01): at a given SOC, the temperature of the cell with higher charging rate is higher and increasing the charge rate results in a greater rise in cell temperature, indicating a greater variation in temperature over time. The data indicates a strong correlation between the simulation results and the experimental measurements, demonstrating good alignment between the two.

Figure 2 shows the results of the first simulation. As discussed, the initial charge of the cell was near zero and it was charged using a 4.5 C current to fully charged state, as can be seen in Figure 2a. As the cell is charging, its temperature increases due to electrochemical reactions. Therefore, due to low capacity and impedance, temperature difference is also low. There is a small difference in the temperature trend in Figure 2b, that can be related to heat dissipation of the cell to the ambient conditions and thermal characteristics of the cell. Also, as can be seen in Figure 2c, the temperature at the center of the cell's core is higher, which is influenced by the geometry of the system.

To find the most influential parameters on temperature and temperature deviation over time, a linear regression method was applied. After feature selection using p-value test with 5% confident range, presented in Table 1, five parameters were identified as the effective factors affecting temperature at 50% SOC: capacity, current, ohmic resistance and two two-way interactions of capacity with current and ohmic resistance. R-squared of the fitted model is 96.55% which shows a very good agreement between predicted and measured values. Based on the reported p-values, a relationship between temperature and parameters such as capacity, current, and ohmic resistance can be established. These factors directly influence the cell's temperature, with higher values of these parameters leading to increased cell temperature.

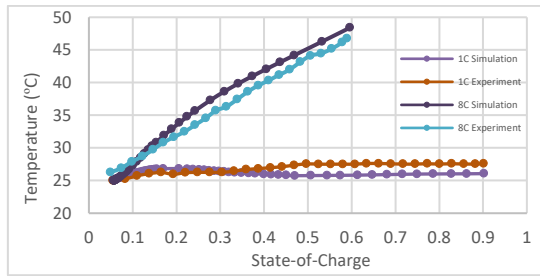


Figure 1: Temperature vs SOC in Charging test for 1C and 8C simulation vs experiment (Dong et al., 2018)

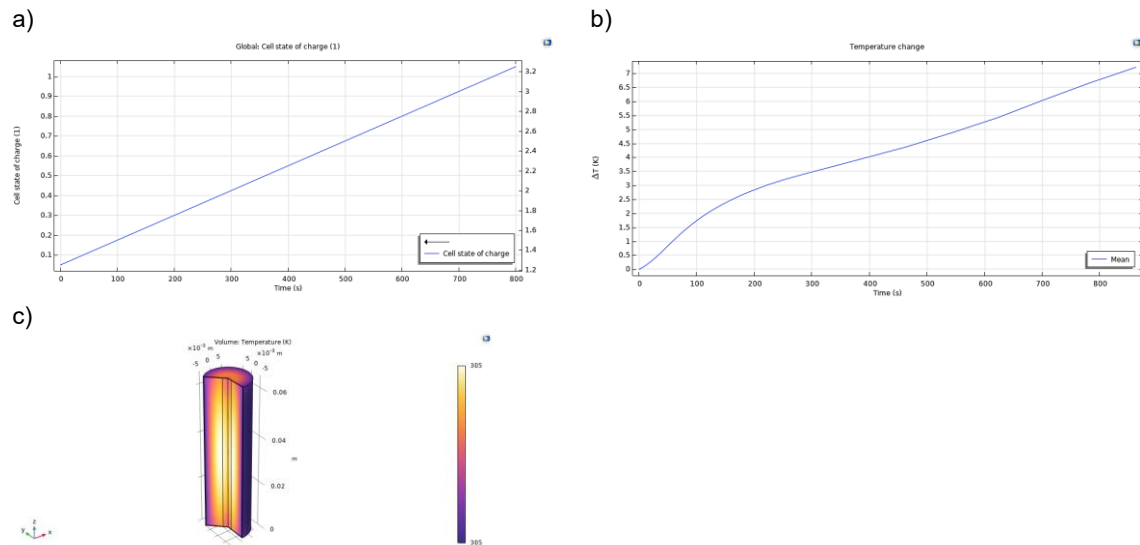


Figure 2 – Simulation of the cell number 1 – 0.5 Ah, 4.5C and 5  $\mu\Omega$  – a) state-of-charge vs time, b) mean temperature deviation of cell vs time and c) Temperature distribution in the cell at 800s

Table 1: P-values for mean temperature at 50 % charge

Source	DF	P-Value
Model	5	0.000
Capacity	1	0.000
Current	1	0.000
Impedance	1	0.010
Capacity*Current	1	0.001
Capacity*Impedance	1	0.027
Error	7	
Total	12	

#### 4. Conclusions

One of the major safety issues in Li-ion cells usage is the thermal runaway which is a catastrophic heat release, with possible ignition and explosion. Most of the studies devoted to understanding the behavior of the cell during a thermal runaway are focused on a fresh and uncycled battery, which has a much better resilience to thermal stress; as already reported in the literature, the capacity and internal resistance of a cycled cell is different from those of a new one. In this study, the influence of these factors was investigated, with specific reference to Ohmic resistance and capacity of the cell and to charging current. The statistical analysis of the results shows a very good agreement between the fitted and measured values, showing a strong relationship between these factors and the temperature of the cell. As can be concluded from the results of the simulation, a faded capacity battery is less prone to go beyond the designed temperature. However, in real-world scenario, an aged cell with faded capacity has a lower life span and battery performance. Furthermore, as battery degrades, the internal resistance will increase, leading to more significant effect on the temperature. Under the same conditions, a cell

with higher ohmic resistance tends to reach a higher temperature due to increased heat generation. As discussed, these two factors can cancel each other out and the objective of the study was set to understand the predominant factor. The statistical analysis showed that the capacity is a more influencing factor. The study insights could guide predictive maintenance schedules, enabling timely interventions and informing actionable strategies to enhance the safety and reliability of energy storage systems in real-world applications.

### Nomenclature

$\rho$ – density, kg/m <sup>3</sup>	$E_{a,i}$ – activation energy of ith side reaction, J/mol
$c_p$ – specific heat capacity, J/kg*K	$\tau$ – the diffusion time constant, s
$T$ – temperature, K or °C	$I$ – current, A
$k$ – Thermal conductivity, W/m*K	$Q$ – cell capacity, Ah
$t$ – time, s	$J$ . dimensionless charge exchange current
$S_i$ – heat generated by ith side reaction, W/m <sup>3</sup>	$R_{ohm}$ - ohmic resistance, mΩ
$L_i$ – thickness of ith part, m	SOC – state-of-charge of the cell
$c_i$ - dimensionless concentration	$F$ – Faraday constant
$R_i$ - reaction rate for the ith side reaction, s <sup>-1</sup>	$\eta$ - Overpotential, V
$W_i$ - specific active substance content of the ith side reaction, kg/m <sup>3</sup>	$D$ – Diffusivity coefficient, m/s
$A_i$ – rate coefficient of ith side reaction, s <sup>-1</sup>	$E_{cell}$ – Voltage of the cell, V
$H_i$ - the reaction heat for the ith side reaction, J/kg	

### Acknowledgments

The results of this work have been obtained with the financial support of the National Recovery and Resilience Plan (PNRR), Mission 4 Component 2 Investment 1.3, funded by the European Union - NextGenerationEU, Spoke 6 "Energy Storage" of the Extended Partnership (PE2) NEST - Network 4 Energy Sustainable Transition.

### References

- Bubbico, R.; Greco, V.; Menale, C., 2018, Hazardous scenarios identification for Li-ion secondary batteries. *Saf. Sci.*, 108, 72–88.
- Cianciullo M., Vilardi G., Mazzarotta B., Bubbico R., 2022, Simulation of the Thermal Runaway Onset in Li-Ion Cells—Influence of Cathode Materials and Operating Conditions, *Energies*, 15, 4169.
- Dong, T., Peng, P., & Jiang, F., 2018, Numerical modeling and analysis of the thermal behavior of NCM lithium-ion batteries subjected to very high C-rate discharge/charge operations. *International journal of heat and mass transfer*, 117, 261-272.
- Doyle, M., Fuller, T. F., & Newman, J., 1993, Modeling of galvanostatic charge and discharge of the lithium/polymer/insertion cell. *Journal of the Electrochemical society*, 140(6), 1526.
- Doyle, M., Newman, J., Gozdz, A. S., Schmutz, C. N., & Tarascon, J. M., 1996, Comparison of modeling predictions with experimental data from plastic lithium ion cells. *Journal of the Electrochemical Society*, 143(6), 1890.
- Ekström, H., Fridholm, B., & Lindbergh, G., 2018, Comparison of lumped diffusion models for voltage prediction of a lithium-ion battery cell during dynamic loads. *Journal of Power Sources*, 402, 296-300.
- Feng, X., Ouyang, M., Liu, X., Lu, L., Xia, Y., & He, X. (2018). Thermal runaway mechanism of lithium ion battery for electric vehicles: A review. *Energy storage materials*, 10, 246-267.
- Guo, M., Sikha, G., & White, R. E., 2010, Single-particle model for a lithium-ion cell: Thermal behavior. *Journal of The Electrochemical Society*, 158(2), A122.
- Guo, Q., Zhang, J., Zhou, C., Huang, Z., & Han, D., 2023, Thermal runaway behaviors and kinetics of NCM lithium-ion batteries at different heat dissipation conditions. *Journal of The Electrochemical Society*, 170(8), 080507.
- Kim, G. H., Pesaran, A., & Spotnitz, R. (2007). A three-dimensional thermal abuse model for lithium-ion cells. *Journal of power sources*, 170(2), 476-489.
- Menale, C., D'Annibale, F., Mazzarotta, B., Bubbico, R. 2019, "Thermal management of lithium-ion batteries: An experimental investigation", *Energy*, vol. 182, pp. 57-71.
- Vetter, J., Novák, P., Wagner, M. R., Veit, C., Möller, K. C., Besenhard, J. O., ... & Hammouche, A. (2005). Ageing mechanisms in lithium-ion batteries. *Journal of power sources*, 147(1-2), 269-281.
- Wang, J., & Azam, W., 2024, Natural resource scarcity, fossil fuel energy consumption, and total greenhouse gas emissions in top emitting countries. *Geoscience Frontiers*, 15(2), 101757.
- Wen, J., Yu, Y., & Chen, C., 2012, A review on lithium-ion batteries safety issues: existing problems and possible solutions. *Materials express*, 2(3), 197-212.